HHS Public Access

Author manuscript

Kidney Int. Author manuscript; available in PMC 2018 July 01.

Published in final edited form as:

Kidney Int. 2017 July ; 92(1): 114–124. doi:10.1016/j.kint.2016.12.023.

Mesenchymal stem cell-derived extracellular vesicles attenuate kidney inflammation

Alfonso Eirin, MD[1], **Xiang-Yang Zhu, MD, PhD**[1], **Amrutesh S. Puranik, PhD**[1], **Hui Tang, MD, PhD**[1], **Kelly A. McGurren**[1], **Andre J. van Wijnen, PhD**[2], **Amir Lerman, MD**[3], and **Lilach O. Lerman, MD, PhD**[1,3]

[1]Division of Nephrology and Hypertension, Mayo Clinic, Rochester, MN

[2]Division of Orthopedic Surgery, Mayo Clinic, Rochester, MN

[3]Division of Cardiovascular Diseases, Mayo Clinic, Rochester, MN

Abstract

Mesenchymal stem/stromal cells (MSCs) have distinct capability for renal repair, but may have safety concerns. MSC-derived extracellular vesicles emerged as a novel non-cellular alternative. Using a porcine model of metabolic syndrome and renal artery stenosis we tested whether extracellular vesicles attenuate renal inflammation, and if this capacity is mediated by their cargo of the anti-inflammatory cytokine interleukin (IL)10. Pigs with metabolic syndrome were studied after 16 weeks of renal artery stenosis untreated or treated four weeks earlier with a single intrarenal delivery of extracellular vesicles harvested from adipose tissue-derived autologous MSCs. Lean and sham metabolic syndrome animals served as controls (seven each). Five additional pigs with metabolic syndrome and renal artery stenosis received extracellular vesicles with pre-silenced IL10 (IL10 knock-down). Single-kidney renal blood flow, glomerular filtration rate, and oxygenation were studied *in vivo* and renal injury pathways *ex vivo*. Retention of extracellular vesicles in the stenotic-kidney peaked two days after delivery and decreased thereafter. Four weeks after injection, extracellular vesicle fragments co-localized with stenotic-kidney tubular cells and macrophages, indicating internalization or fusion. Extracellular vesicle delivery attenuated renal inflammation, improved medullary oxygenation and fibrosis. Renal blood flow and glomerular filtration rate fell in metabolic syndrome and renal artery stenosis compared to metabolic syndrome, but was restored in pigs treated with extracellular vesicles. These renoprotective effects were blunted in pigs treated with IL10-depleted extracellular vesicles. Thus, extracellular vesicle-based regenerative strategies might be useful for patients with metabolic syndrome and renal artery stenosis.

Correspondence: Lilach O. Lerman, MD, PhD, Division of Nephrology and Hypertension, Mayo Clinic, 200 First Street SW, Rochester, MN, 55905. Lerman.Lilach@Mayo.Edu, Phone: (507)-266-9376, Fax: (507)-266-9316.

DISCLOSURE

All the authors declare no competing interests.

Keywords

metabolic syndrome; renal artery stenosis; mesenchymal stem cells; extracellular vesicles; interleukin-10

INTRODUCTION

Advances in regenerative medicine have uncovered a distinct potential of mesenchymal/stromal cells (MSCs) for kidney repair[1], which resides in their remarkable anti-inflammatory and immunomodulatory properties. We have previously shown that intra-renal delivery of autologous adipose tissue-derived MSCs decreased inflammation and improved function in the stenotic-kidney of pigs with non-atherosclerotic renal artery stenosis (RAS)[2, 3] or with atherosclerotic RAS undergoing revascularization[4, 5]. However, concerns regarding safety and transplantation of viable replicating cells, such as induction of tumors, malformations, or microinfarctions, may limit their translational capacity[6].

MSCs are avid producers of extracellular vesicles (EVs), including microvesicles (50–1000nm in size), formed by outward budding and fission of the plasma membrane, and exosomes (40–100nm), formed in multi-vesicular bodies and released upon fusion with the membrane[7]. MSC-derived EVs shuttle functional components capable of reducing tissue injury and/or enhancing repair in recipient cells, thereby mediating MSC paracrine action[8]. We have recently shown that cultured porcine adipose tissue-derived MSCs release EVs that contain genes and proteins capable of modulating inflammation, angiogenesis, adipogenesis, and other pathways in recipient cells[9, 10]. Indeed, delivery of EVs derived from MSCs has been shown to restore renal structure and function in experimental rodent models of acute renal failure[11–14]. However, their ability to rescue kidney function in chronic renal injury in a large preclinical animal model is unknown. Moreover, the mechanisms associated with MSC-derived EV renoprotective effect remain to be defined.

Interleukin (IL)-10 is an anti-inflammatory cytokine that regulates the functions of immune cells, and a key determinant of “alternatively” activated (M2) macrophage phenotype. Macrophages can change their expression profile in response to insults, and their effector phenotype determines the nature and severity of renal injury[15]. “Classically” activated (M1) macrophages express pro-inflammatory cytokines, whereas M2 macrophages attenuate inflammation and promote tissue repair. We have previously shown that IL-10 expression is blunted in both porcine[2] and human[16] stenotic kidneys, and correlates inversely with tubular injury score and renal fibrosis[17]. Furthermore, MSC delivery into the stenotic kidney favored a phenotypic switch from M1 to M2 macrophages and improved IL-10 expression, as well as renal function and structure[2, 3], suggesting that this cytokine might be implicated in the MSC-induced reparative process. However, whether IL-10 mediates the paracrine actions of the MSC progeny EVs to preserve kidneys subjected to chronic ischemia has not been directly explored.

The current study took advantage of a novel porcine model of coexisting metabolic syndrome (MetS) and RAS (MetS+RAS), comorbidities that accentuate renal inflammation, associated with prominent glomerular and tubular alterations[18]. We studied the temporal

pattern of EV uptake and distribution, and tested the hypothesis that intra-renal delivery of autologous MSC-derived EVs would attenuate inflammation, ameliorating structural and functional decline in the MetS+RAS kidney. Furthermore, we tested whether the renoprotective properties of EVs are partly determined by their cargo of IL-10.

RESULTS

MetS+RAS

MetS+RAS was achieved by inducing unilateral RAS in domestic pigs 6 weeks after initiating a high cholesterol/carbohydrate diet. MetS pigs were studied in-vivo and ex-vivo after 10 weeks of RAS untreated or treated 4 weeks earlier with a single intrarenal delivery of EVs harvested from autologous adipose tissue-derived MSCs, or saline vehicle (Figure 1A). The systemic characteristics in all pigs 4 weeks after EV delivery or sham are summarized in Table 1. Body weight and blood pressure were similarly higher in all MetS groups compared to Lean. All RAS groups developed a moderate but significant stenosis of a similar degree ($p>0.05$ ANOVA). Common to the chronic phase of untreated RAS, plasma renin activity (PRA) levels were similar among the groups. Lipid fraction levels were comparably elevated in all MetS groups compared to Lean, and their fasting insulin and homeostasis model assessment of insulin resistance (HOMA-IR) levels were significantly higher. Yet, fasting glucose levels did not differ among the groups, indicating non-diabetic MetS[19].

MSC and EV characterization

Cultured MSCs expressed typical markers, and trans-differentiated into osteocytes, chondrocytes, and adipocytes, as typical to MSC[3, 4, 20]. Transmission and scanning electron microscopy demonstrated that they secreted substantial amounts of EVs (Figure 1B). NanoSight analysis revealed that 10×10ˆ6 MSCs/kg cultured for 72hr released 1×10ˆ10 EVs/ml. Their size distribution indicated that MSC-derived EVs included about 2/3 small microvesicles (~150 nm in size) and 1/3 exosomes (~50 nm) (Figure 1C), and Western blotting demonstrated expression of characteristic EV and MSC markers (Figure 1D).

EVs engrafted and decreased inflammation in the stenotic kidney

EVs were labeled with a red fluorescent dye and subsequently injected into the stenotic renal artery. Pigs were euthanized at time intervals after intra-renal EV injection. Labeled EVs were tracked in frozen sections from the heart, lungs, liver, spleen, and both kidneys, and their retention calculated. Retention of EVs in the stenotic kidney peaked at 2 days (~9% of injected amount) and decreased thereafter, remaining at ~2% by 4 weeks after injection (Figure 2D). Other initial major retention sites included the liver, lung, and spleen (peaking at 45%, 40%, and 15%, respectively). EVs were also detected in small proportion in the heart and contralateral kidney.

Four weeks after intra-renal administration, red fluorescent signal was detected within the damaged kidney, but not in stenotic kidney sections of untreated animals (Figure 2A). To determine the nature of the red fluorescent signal, we performed immunofluorescence staining with antibodies against exosome (CD9) and microvesicle (CD63) markers. Only a

fraction of red-stained particles co-localized with CD9, and none with CD63 (Figure 2B), Suggesting that the red fluorescent signal was attributable to EV fragments rather than intact EVs retained within cells. EV Fragments co-localized with phaseolus vulgaris erythroagglutinin (PHA-E+), peanut agglutinin (PA+), and CD68+, suggesting EV engraftment in proximal and distal tubular cells, as well as macrophages (Figure 2C).

The number of infiltrating inflammatory M1 macrophages, which was higher in MetS compared to Lean kidneys, further increased in MetS+RAS, but decreased in MetS+RAS +EVs pigs (Figure 3A–B). In contrast, fewer reparative M2 macrophages were observed in MetS and MetS+RAS compared to Lean kidneys, but their number was normalized in EV-treated pigs (Figure 3A–C). Consequently, M1/M2 ratio, higher in MetS compared to Lean, further increased in MetS+RAS, but decreased in MetS+RAS+EVs pigs (Figure 3D).

Macrophages exacerbate renal injury by secreting pro-inflammatory cytokines. In blood samples collected from the renal vein, levels of the pro-inflammatory cytokines monocyte-chemoattractant protein (MCP)-1, tumor necrosis factor (TNF)-α, IL-6, and IL-1β were elevated in MetS+RAS, but decreased in MetS+RAS+EVs pigs (Figure 4A). Conversely, both renal vein levels and tissue immunoreactivity of IL-10 were reduced in MetS and MetS +RAS compared to Lean, but normalized in MetS+RAS+EVs (Figure 4AB). Tubulointerstitial IL-4 co-localized with IL-10, and similar to IL-10 its immunoreactivity was reduced in MetS compared to Lean, further decreased in MetS+RAS, but normalized in MetS+RAS+EVs (Figure 4B).

EVs attenuated renal hypoxia and fibrosis

Production of pro-inflammatory cytokines can evoke renal hypoxia and fibrosis. Medullary hypoxia assessed using blood-oxygen-level-dependent (BOLD)-MRI showed similarly elevated BOLD-R2* index in MetS and MetS+RAS, which decreased to normal levels in MetS+RAS+EVs (Figure 5A–B). Tubulo-interstitial fibrosis (trichrome staining) increased in MetS+RAS compared to Lean and MetS, and slightly but significantly decreased in MetS +RAS+EVs (Figure 5A–C), as did glomerular score (Figure 5D).

EVs restored renal function

Renal hemodynamics and function were assessed with multi-detector CT (MDCT). Single-kidney volume, RBF and GFR, which were higher in all MetS compared to Lean, decreased in MetS+RAS, but did not differ from MetS in EV-treated MetS+RAS pigs (Table 1). Serum creatinine also normalized in MetS+RAS+EVs.

EV renoprotective effects were blunted by IL10 knock-down (IL10KD)

IL10 mRNA expression was 100-fold higher in EVs compared to their parent MSCs (Figure 6A), and IL-4 protein expression was enriched (Figure 6B). To establish the role of IL10 in mediating the renoprotective effect of MSC-derived EVs, MSCs were incubated with siRNA for this anti-inflammatory cytokine. The resultant IL10KD MSCs were characterized by decreased IL10 mRNA and protein expression (Figure 6C–D), and their daughter IL10KD-EVs by lower IL10 mRNA expression (Figure 6E).

These IL10KD-EVs were then delivered into the renal artery of 5 additional MetS+RAS pigs. Four weeks later stenotic-kidney volume, RBF, and GFR, which all improved in MetS +RAS+EVs, were not different from those in untreated MetS+RAS (Table 1), and serum creatinine showed a similar pattern (Table 1). The number of M1 and their ratio to M2 macrophages in the kidney failed to decline (Figure 3A–D), and renal vein levels and tissue immunoreactivity of IL-10 and IL-4 that improved in MetS+RAS+EVs remained downregulated in MetS+RAS+IL10KD-EVs (Figure 4A–B). Furthermore, renal vein levels of MCP-1, TNF-α, IL-6, and IL-1β that decreased in MetS+RAS+EVs also remained upregulated in MetS+RAS+IL10KD-EVs (Figure 4A). Lastly, medullary hypoxia, tubulo-interstitial fibrosis, and glomerular score were not attenuated in MetS+RAS+IL10KD-EVs (Figure 5A–D).

DISCUSSION

Our study demonstrates that a single intra-renal delivery of MSC-derived EVs improves renal structure and function in experimental MetS+RAS. Restoration of stenotic-kidney GFR was associated with decreased inflammation, medullary hypoxia, and fibrosis, positioning EVs as a novel therapeutic approach to ameliorate chronic renal injury and dysfunction induced by coexisting MetS and RAS. Furthermore, our study suggests that at least some of the salutary effects of EVs are mediated by their cargo of IL-10, as they were abolished in MetS+RAS+IL-10KD-EV-treated pigs.

MSCs possess potent anti-inflammatory and immunomodulatory properties, which render them an attractive tool to attenuate kidney damage[1]. We have shown in porcine atherosclerotic and non-atherosclerotic RAS that MSC delivery reduced inflammation and restored function in the post-stenotic kidney[2–5]. The current study extends our previous observations, demonstrating that stenotic kidney structure and function are also preserved four weeks after delivery of MSC-derived EVs, This tool may therefore be useful, as EVs circumvent concerns about extensive expansion, cryopreservation, complications, and mal-differentiation of live replicating MSC.

MSCs produce large amount of EVs that can be internalized into other cells and activate anti-inflammatory signaling by delivering protein and genetic content[7, 8]. We have previously found that EVs emanating from porcine MSCs contain mRNA and proteins that regulate several cellular pathways[9, 10]. Furthermore, incorporation of MSC-derived EVs in acutely injured renal proximal tubular cells modulates the expression of genes involved in cell recovery and repair by shuttling mRNA involved in transcription, proliferation, and immunoregulation[11]. However, their efficacy in chronic renal injury remained unclear.

To test the in-vivo efficacy of MSC-derived EVs, we utilized a novel domestic porcine model of MetS+RAS that replicates human disease conditions. We have previously shown in obese Ossabaw pigs that MetS induces renal inflammation and microvascular loss[21], which were aggravated by superimposition of RAS[18]. Given these characteristics of the stenotic MetS kidney, we selected the porcine MetS+RAS model to test the efficacy of MSC-derived EVs to ameliorate chronic renal injury. This study shows that MSCs isolated from porcine adipose tissue release EVs that express typical EV and MSC markers. While similar to other

nanoparticles the majority of these EV might be taken up by the reticuloendothelial system[22], at 2 days after injections up to 10% were observed within the stenotic kidney. By 4 weeks their stenotic kidney retention declined to ~2%, yet their beneficial effects lingered.

We found that four weeks after delivery, EV fragments co-stained with CD68, suggesting uptake by macrophages, or were retained within PA+ and PHA-E+ cells, suggesting incorporation into proximal and distal tubules. Only a small fraction of EVs remained intact four weeks after administration, denoted by red-labeled particles co-localizing with EV markers. Taken together, these observations are consistent with the postulated capability of EVs to be internalized, and potentially transfer their content to recipient cells[11].

Notably, internalization of MSC-derived EVs by macrophages was accompanied by reduced renal inflammation, a major pathological characteristic of MetS that mediates many of its harmful sequelae. We have previously detected elevated renal vein levels of pro-inflammatory cytokines in the post-stenotic human kidney, associated with decreased renal function, underscoring the contribution of inflammation to kidney injury[16, 23]. Additionally, we have demonstrated in obese Ossabaw pigs predominance of pro-inflammatory (M1) compared to trophic (M2) macrophages populating the stenotic kidney[18], providing the impetus for targeted therapies to prevent post-stenotic M1 macrophage accumulation and/or drive the phenotypic shift to M2 macrophages. MSCs appear to be suitable for this purpose, as their co-culture with activated monocytes or delivery into the porcine RAS kidney decrease M1 and increase M2 marker expression[2]. The current study extends these observations and underscores the ability of MSC-derived EV progeny to reverse chronic MetS+RAS-induced renal inflammation, evidenced by a phenotypic switch of macrophages from M1 to M2, which is likely mediated by IL-10. Indeed, renal expression of the M2 cytokine IL-10, which was downregulated in MetS and MetS+RAS, normalized in EV-treated pigs. Likewise, immunoreactivity of IL-4, which was also enriched in EVs, normalized in MetS+RAS+EVs, supporting its role in mediating macrophage polarization towards an M2 phenotype[24]. Furthermore, EV delivery decreased renal vein levels of the M1 pro-inflammatory cytokines TNF-α, IL-1β, and IL-6, as well as renal vein levels of MCP-1, a pro-inflammatory cytokine that mediates M1 macrophage recruitment[25]. Conceivably, the anti-inflammatory effect of EVs on the MetS+RAS kidney might be related to their internalization not only by macrophages, but also by tubular cells, which produce inflammatory cytokines that contribute to macrophage polarization[26].

In this study, MetS+RAS-induced renal inflammation was associated with increased medullary hypoxia, a condition that triggers a vicious cycle of progressive kidney injury and fibrosis, and represents a common pathway to end-stage renal disease[27]. Inflammation and hypoxia are closely linked by an increase in cellular metabolic demand and oxidative stress[28]. Activation of inflammatory pathways within the stenotic kidney, including macrophage accumulation and subsequent release of inflammatory cytokines, has been implicated in the development of hypoxia in the medulla[29], which is particularly vulnerable to hypoxia. Indeed, we found that medullary hypoxia was elevated in MetS and MetS+RAS groups, but decreased in pigs treated with MSC-derived EVs, possibly due to their ability to reduce renal inflammation.

Furthermore, MetS+RAS-induced fibrosis was attenuated in EV-treated pigs, likely secondary to amelioration of inflammation. Macrophage infiltrates are common in stenotic kidneys of RAS patients with reduced RBF and correlate with tubular atrophy and fibrosis[30]. Glomerulosclerosis also decreased in MetS+RAS+EVs, suggesting that EVs confer tubular and glomerular protection. Congruently, stenotic-kidney RBF was diminished in MetS+RAS compared to MetS, but increased in MetS+RAS+EVs, associated with increased renal function, reflected as decreased serum creatinine and increased stenotic-kidney GFR. Incidentally, restoration of RBF and GFR to levels comparable to MetS might hypothetically reflect restoration of renal hyperfiltration. Nevertheless, this was associated with several beneficial effects conferred by EVs in the stenotic MetS kidney, such as decreased inflammation, fibrosis, and glomerulosclerosis, underscoring the potential of this intervention to mitigate renal injury. Further studies are needed to determine the long-term effect of this maneuver in MetS.

Given the prominent inflammatory component and predominance of M1 macrophages in MetS+RAS, we tested the role of the EV cargo of IL-10 in their beneficial effects. This anti-inflammatory cytokine has been shown to modulate renal repair in mice with ischemia-reperfusion injury[31]. Furthermore, IL-10-deficient mice with glomerulonephritis develop histologically and functionally more severe renal injury than wild-type mice, implying that IL-10 regulates many aspects of renal function[32]. In this study, we found that EVs were markedly enriched with IL10 mRNA compared to their parent MSCs, and when incorporated into renal cells, upregulated IL-10 renal expression. IL-10 silencing decreased its mRNA and protein expression in MSC, and increased renal release of pro-inflammatory cytokines and M1/M2 macrophage ratio. Notably, many of the renoprotective effects of EVs were blunted in pigs treated with IL10-depleted EVs, underscoring the role of this anti-inflammatory cytokine in mediating EV-induced renal recovery. Interestingly, IL-10 silencing decreased IL-4 immunoreactivity and increased M1/M2 ratio, suggesting that these cytokines may act in concert to induce a phenotypic switch of macrophages from M1 to M2. Further studies are needed to explore the interaction between IL-10 and IL-4 in the post-stenotic kidney.

Remarkably, intra-renal administration of IL10 KD EVs had a profound effect on GFR, which became significantly lower than that of MetS+RAS. The mechanisms by which IL-10 deficiency decreased GFR remain elusive, but IL10 is known to counterbalance inflammatory cytokines, which remain unopposed in its absence[33]. In turn, renal hypoxia and elevated release of inflammatory markers may trigger parenchymal injury and interfere with renal functional recovery[17]. In the current study, we found that treatment with IL10KD-EVs aggravated medullary hypoxia, inflammation, and fibrosis, which are all important determinants of GFR. Therefore, alterations in these pathways may partly explain the profound effect on GFR seen in IL10KD EV-treated pigs.

Our study is limited by the short duration of MetS and RAS and by the use of relatively young pigs, which might influence their interaction with pathological factors involved in disease progression. Our MetS pigs developed obesity, hyperlipidemia, glucose intolerance (as per HOMA-IR), and hypertension, yet superimposition of RAS did not further increase blood pressure, possibly due to the relatively moderate nature of the stenosis. Importantly,

post-stenotic injury and dysfunction in our porcine model closely mimic those observed in humans[30]. The mechanisms regulating EV engraftment remain to be determined, but speculatively damaged tubular cells might express cognate ligands and receptors to enhance their uptake. Indeed, we found that EVs expressed the surface receptors CD9, CD29, and CD63, adhesion molecules that facilitate EV incorporation into cells[34]. Yet, phagocytosis might be the primary mechanism responsible for EV internalization into macrophages. Future research is needed to develop strategies to augment renal EV uptake and retention.

In summary, our study identified a potency of EVs isolated from adipose tissue-derived MSCs for ameliorating renal injury in chronic experimental MetS+RAS. Intra-renal delivery of MSC-EVs decreased renal inflammation, increased the number of reparative macrophages, and upregulated expression of IL-10, suggesting that anti-inflammatory properties underpin the protective effects of EVs on the stenotic-kidney. Furthermore, EVs attenuated renal fibrosis, ultimately improving stenotic kidney function. Notably, their beneficial effects were blunted in MetS+RAS pigs that received IL10KD-EVs, supporting an important contribution of this cytokine to several aspects of renal function. The current study is therefore an important step before clinical translation of this tool. Future studies are needed to establish the long-term effects, optimal timing, and dose of EVs, and determine their efficacy in humans.

MATERIALS AND METHODS

The Institutional Animal Care and Use Committee approved this study. Thirty-three domestic female pigs were studied during 16wks of observation. At baseline, 26 pigs started high-cholesterol/high carbohydrate diet (MetS)[19], while 7 were fed regular pig chow (Lean).

Six weeks later, animals were anesthetized with 0.25g of IM tiletamine hydrochloride/ zolazepam hydrochloride and 0.5g of xylazine, and maintained with intravenous ketamine (0.2mg/kg/min) and xylazine (0.03mg/kg/min). RAS was induced in 19 MetS pigs by placing a local-irritant coil in the main renal artery[35]. Sham renal angiography was performed in 7 Lean and 7 MetS pigs. In all animals randomized to receive EVs, fat tissue was collected at that time, which was subsequently used to harvest autologous MSCs and isolate their EVs.

Six weeks later, the degree of stenosis was determined by angiography. EVs (1×10ˆ10) were pre-harvested from the autologous adipose-tissue-derived MSCs, dose commonly used for intra-renal delivery. EVs with (n=5) or without (n=7) pre-silenced IL-10 were suspended in PBS and injected into the stenotic kidney of MetS+RAS over 5min through a 5F catheter positioned proximal to the stenosis.

Four weeks later, pigs were again similarly anesthetized, systemic blood samples collected for lipid panels, PRA, and serum creatinine measurements. Fasting glucose and insulin levels were measured by standard procedures, and the HOMA-IR calculated as an index of insulin resistance[19]. Single-kidney hemodynamics and function were assessed using MDCT and oxygenation by BOLD-MRI.

One week after later, animals were euthanized with an intravenous bolus of 100mg/kg of sodium pentobarbital[36]. The stenotic or right kidneys were dissected, and sections frozen in liquid nitrogen (and maintained at −80°C) or preserved in formalin for ex-vivo studies.

In-vivo studies

BOLD MRI studies were performed on a 3 Tesla to measure intra-renal oxygenation (R2*), as previously described[5, 21, 37, 38].

MDCT scanning was performed to assess single-kidney volume, regional perfusion, RBF, and GFR, as shown[17, 39–41].

Ex-vivo studies

MSC and EV isolation, characterization, and culture—Abdominal subcutaneous adipose tissue (5–10g) was collected from pigs 4wks after induction of RAS or sham, processed for MSC isolation using collagenase, and cultured with advanced MEM medium supplemented with platelet lysate[42]. MSCs were kept in cell recovery medium for phenotype/function analysis. MSCs were characterized by the expression of CD44, CD90, and CD105, and lack of expression of CD45, CD34, CD14 surface molecules using immunofluorescent staining and flow-cytometry[4, 9, 43]. MSC characterization was confirmed by their trans-differentiation into to adipocytes, chondrocytes, and osteocytes, as described[3, 4, 20]. Transmission and scanning electron microscopy was performed to investigate size and structure of MSC-derived EVs.

EVs were obtained from supernatants of 10×10ˆ6 MSCs, cultured in advanced MEM medium without supplements, and ultra-centrifuged twice, as shown[9]. 75,000 cells release approximately 15μg of EVs overnight (Figure 1B). Briefly, after centrifugation at 2000g, supernatants were ultra-centrifuged at 100,000g, washed in serum-free medium 199 containing HEPES 25mM, and underwent a second ultra-centrifugation. Pellets were suspended, and protein content quantified. Endotoxin contamination was excluded by Limulus testing, and EVs stored at −80°C[11]. Concentration and size distribution of isolated EVs was assessed by nanoparticle tracking analysis. EVs from MSCs were then characterized based on the expression of the EV (CD9, CD29, CD63) and MSC (CD73, CD105) markers by Western blot. EV and MSC mRNA content of IL-10 were measured by real time PCR using spike-in methods (luciferase control mRNA as exogenous RNA). In addition, IL10 and IL4 protein expression was measured by by Western blot[2].

EV tracking and tissue distribution—EVs were labeled prior to delivery with the red fluorescence PKH26. Their localization was evaluated in 5μm stenotic kidney sections by immunofluorescence staining with the exosome marker CD9, the microvesicle marker CD63, the distal tubular marker PA, the proximal tubular marker PHA-E, and the macrophage marker CD68[43].

In addition, we assessed biodistribution of MSC-derived EVs in 8 additional pigs euthanized 3h, 2d, 7d, or 4wks after intrarenal EV injection (n=2 each). Labeled EVs were tracked and counted in frozen sections from the heart, lungs, liver, spleen, and both kidneys, and their relative retention calculated at each time point and expressed as % of injected amount.

Renal injury pathways—Renal inflammation was evaluated by immunostaining with antibodies detecting CD68+/inducible nitric oxide synthase (iNOS)+ (M1) and CD68+/Arginase-1+ (M2) macrophages[2]. Renal vein levels of MCP-1 were measured by ELISA[17], and TNF-α, IL-6, IL-1β, and IL-10 levels by Luminex. Renal expression of IL-10 and IL-4 was measured by immunofluorescent staining. Tubulo-interstitial fibrosis and glomerular score were quantified in renal sections stained with Masson's trichrome[44].

Statistical methods

Statistical analysis was performed using JMP (SAS). Results were expressed as mean±SD or median (interquartile range). Parametric (ANOVA/Student t-test) and nonparametric (Wilcoxon/Kruskal-Wallis) tests were used as appropriate. $P<0.05$ was considered statistically significant.

Supplementary Material

Refer to Web version on PubMed Central for supplementary material.

Acknowledgments

This study was partly supported by NIH grant numbers DK102325, DK73608, DK104273, HL123160, and DK106427, and by the Mayo Clinic Center for Regenerative Medicine.

References

1. Eirin A, Lerman LO. Mesenchymal stem cell treatment for chronic renal failure. Stem Cell Res Ther. 2014; 5:83. [PubMed: 25158205]
2. Eirin A, Zhang X, Zhu XY, et al. Renal vein cytokine release as an index of renal parenchymal inflammation in chronic experimental renal artery stenosis. Nephrol Dial Transplant. 2014; 29:274–282. [PubMed: 24097799]
3. Zhu XY, Urbieta-Caceres V, Krier JD, et al. Mesenchymal stem cells and endothelial progenitor cells decrease renal injury in experimental swine renal artery stenosis through different mechanisms. Stem Cells. 2013; 31:117–125. [PubMed: 23097349]
4. Eirin A, Zhu XY, Krier JD, et al. Adipose tissue-derived mesenchymal stem cells improve revascularization outcomes to restore renal function in swine atherosclerotic renal artery stenosis. Stem Cells. 2012; 30:1030–1041. [PubMed: 22290832]
5. Ebrahimi B, Eirin A, Li Z, et al. Mesenchymal stem cells improve medullary inflammation and fibrosis after revascularization of swine atherosclerotic renal artery stenosis. PLoS One. 2013; 8:e67474. [PubMed: 23844014]
6. Kunter U, Rong S, Boor P, et al. Mesenchymal stem cells prevent progressive experimental renal failure but maldifferentiate into glomerular adipocytes. J Am Soc Nephrol. 2007; 18:1754–1764. [PubMed: 17460140]
7. Yeo RW, Lai RC, Zhang B, et al. Mesenchymal stem cell: an efficient mass producer of exosomes for drug delivery. Adv Drug Deliv Rev. 2013; 65:336–341. [PubMed: 22780955]
8. Lai RC, Chen TS, Lim SK. Mesenchymal stem cell exosome: a novel stem cell-based therapy for cardiovascular disease. Regen Med. 2011; 6:481–492. [PubMed: 21749206]
9. Eirin A, Riester SM, Zhu XY, et al. MicroRNA and mRNA cargo of extracellular vesicles from porcine adipose tissue-derived mesenchymal stem cells. Gene. 2014; 551:55–64. [PubMed: 25158130]
10. Eirin A, Zhu XY, Puranik AS, et al. Comparative proteomic analysis of extracellular vesicles isolated from porcine adipose tissue-derived mesenchymal stem/stromal cells. Sci Rep. 2016; 6:36120. [PubMed: 27786293]

11. Bruno S, Grange C, Deregibus MC, et al. Mesenchymal stem cell-derived microvesicles protect against acute tubular injury. J Am Soc Nephrol. 2009; 20:1053–1067. [PubMed: 19389847]
12. Bonventre JV. Microvesicles from mesenchymal stromal cells protect against acute kidney injury. J Am Soc Nephrol. 2009; 20:927–928. [PubMed: 19389839]
13. Bruno S, Grange C, Collino F, et al. Microvesicles derived from mesenchymal stem cells enhance survival in a lethal model of acute kidney injury. PLoS One. 2012; 7:e33115. [PubMed: 22431999]
14. Collino F, Bruno S, Incarnato D, et al. AKI Recovery Induced by Mesenchymal Stromal Cell-Derived Extracellular Vesicles Carrying MicroRNAs. J Am Soc Nephrol. 2015
15. Ricardo SD, van Goor H, Eddy AA. Macrophage diversity in renal injury and repair. J Clin Invest. 2008; 118:3522–3530. [PubMed: 18982158]
16. Eirin A, Gloviczki ML, Tang H, et al. Inflammatory and injury signals released from the post-stenotic human kidney. Eur Heart J. 2013; 34:540–548a. [PubMed: 22771675]
17. Eirin A, Ebrahimi B, Zhang X, et al. Changes in glomerular filtration rate after renal revascularization correlate with microvascular hemodynamics and inflammation in Swine renal artery stenosis. Circ Cardiovasc Interv. 2012; 5:720–728. [PubMed: 23048054]
18. Zhang X, Li ZL, Woollard JR, et al. Obesity-metabolic derangement preserves hemodynamics but promotes intrarenal adiposity and macrophage infiltration in swine renovascular disease. Am J Physiol Renal Physiol. 2013; 305:F265–276. [PubMed: 23657852]
19. Pawar AS, Zhu XY, Eirin A, et al. Adipose tissue remodeling in a novel domestic porcine model of diet-induced obesity. Obesity (Silver Spring). 2015; 23:399–407. [PubMed: 25627626]
20. Eirin A, Zhu XY, Ferguson CM, et al. Intra-renal delivery of mesenchymal stem cells attenuates myocardial injury after reversal of hypertension in porcine renovascular disease. Stem Cell Res Ther. 2015; 6:7. [PubMed: 25599803]
21. Li Z, Woollard JR, Wang S, et al. Increased glomerular filtration rate in early metabolic syndrome is associated with renal adiposity and microvascular proliferation. Am J Physiol Renal Physiol. 2011; 301:F1078–1087. [PubMed: 21775485]
22. You J, Zhou J, Zhou M, et al. Pharmacokinetics, clearance, and biosafety of polyethylene glycol-coated hollow gold nanospheres. Part Fibre Toxicol. 2014; 11:26. [PubMed: 24886070]
23. Eirin A, Gloviczki ML, Tang H, et al. Chronic renovascular hypertension is associated with elevated levels of neutrophil gelatinase-associated lipocalin. Nephrol Dial Transplant. 2012; 27:4153–4161. [PubMed: 22923545]
24. Zhao XN, Li YN, Wang YT. Interleukin-4 regulates macrophage polarization via the MAPK signaling pathway to protect against atherosclerosis. Genet Mol Res. 2016; 15
25. Zhu XY, Chade AR, Krier JD, et al. The chemokine monocyte chemoattractant protein-1 contributes to renal dysfunction in swine renovascular hypertension. J Hypertens. 2009; 27:2063–2073. [PubMed: 19730125]
26. Wang Y, Chang J, Yao B, et al. Proximal tubule-derived colony stimulating factor-1 mediates polarization of renal macrophages and dendritic cells, and recovery in acute kidney injury. Kidney Int. 2015; 88:1274–1282. [PubMed: 26422503]
27. Tanaka T, Nangaku M. The role of hypoxia, increased oxygen consumption, and hypoxia-inducible factor-1 alpha in progression of chronic kidney disease. Curr Opin Nephrol Hypertens. 2010; 19:43–50. [PubMed: 19779337]
28. Eltzschig HK, Carmeliet P. Hypoxia and inflammation. N Engl J Med. 2011; 364:656–665. [PubMed: 21323543]
29. Saad A, Herrmann SM, Textor SC. Chronic renal ischemia in humans: can cell therapy repair the kidney in occlusive renovascular disease? Physiology (Bethesda). 2015; 30:175–182. [PubMed: 25933818]
30. Gloviczki ML, Keddis MT, Garovic VD, et al. TGF expression and macrophage accumulation in atherosclerotic renal artery stenosis. Clin J Am Soc Nephrol. 2013; 8:546–553. [PubMed: 23258796]
31. Wan X, Huang WJ, Chen W, et al. IL-10 deficiency increases renal ischemia-reperfusion injury. Nephron Exp Nephrol. 2014; 128:37–45. [PubMed: 25376659]

32. Kitching AR, Tipping PG, Timoshanko JR, et al. Endogenous interleukin-10 regulates Th1 responses that induce crescentic glomerulonephritis. Kidney Int. 2000; 57:518–525. [PubMed: 10652028]
33. Brito-Melo GE, Peruhype-Magalhaes V, Teixeira-Carvalho A, et al. IL-10 produced by CD4+ and CD8+ T cells emerge as a putative immunoregulatory mechanism to counterbalance the monocyte-derived TNF-alpha and guarantee asymptomatic clinical status during chronic HTLV-I infection. Clin Exp Immunol. 2007; 147:35–44. [PubMed: 17177961]
34. Mulcahy LA, Pink RC, Carter DR. Routes and mechanisms of extracellular vesicle uptake. J Extracell Vesicles. 2014; 3
35. Lerman LO, Schwartz RS, Grande JP, et al. Noninvasive evaluation of a novel swine model of renal artery stenosis. J Am Soc Nephrol. 1999; 10:1455–1465. [PubMed: 10405201]
36. Eirin A, Williams BJ, Ebrahimi B, et al. Mitochondrial targeted peptides attenuate residual myocardial damage after reversal of experimental renovascular hypertension. J Hypertens. 2014; 32:154–165. [PubMed: 24048008]
37. Ebrahimi B, Gloviczki M, Woollard JR, et al. Compartmental analysis of renal BOLD MRI data: introduction and validation. Invest Radiol. 2012; 47:175–182. [PubMed: 22183077]
38. Ebrahimi B, Li Z, Eirin A, et al. Addition of endothelial progenitor cells to renal revascularization restores medullary tubular oxygen consumption in swine renal artery stenosis. Am J Physiol Renal Physiol. 2012; 302:F1478–1485. [PubMed: 22419692]
39. Chade AR, Zhu X, Lavi R, et al. Endothelial progenitor cells restore renal function in chronic experimental renovascular disease. Circulation. 2009; 119:547–557. [PubMed: 19153272]
40. Zhu XY, Chade AR, Rodriguez-Porcel M, et al. Cortical microvascular remodeling in the stenotic kidney: role of increased oxidative stress. Arterioscler Throm Vasc Biol. 2004; 24:1854–1859.
41. Krier JD, Ritman EL, Bajzer Z, et al. Noninvasive measurement of concurrent single-kidney perfusion, glomerular filtration, and tubular function. Am J Physiol Renal Physiol. 2001; 281:F630–638. [PubMed: 11553509]
42. Blande IS, Bassaneze V, Lavini-Ramos C, et al. Adipose tissue mesenchymal stem cell expansion in animal serum-free medium supplemented with autologous human platelet lysate. Transfusion (Paris). 2009; 49:2680–2685.
43. Eirin A, Zhu XY, Ebrahimi B, et al. Intrarenal Delivery of Mesenchymal Stem Cells and Endothelial Progenitor Cells Attenuates Hypertensive Cardiomyopathy in Experimental Renovascular Hypertension. Cell Transplant. 2015; 24:2041–2053. [PubMed: 25420012]
44. Eirin A, Zhu XY, Li Z, et al. Endothelial outgrowth cells shift macrophage phenotype and improve kidney viability in swine renal artery stenosis. Arterioscler Throm Vasc Biol. 2013; 33:1006–1013.

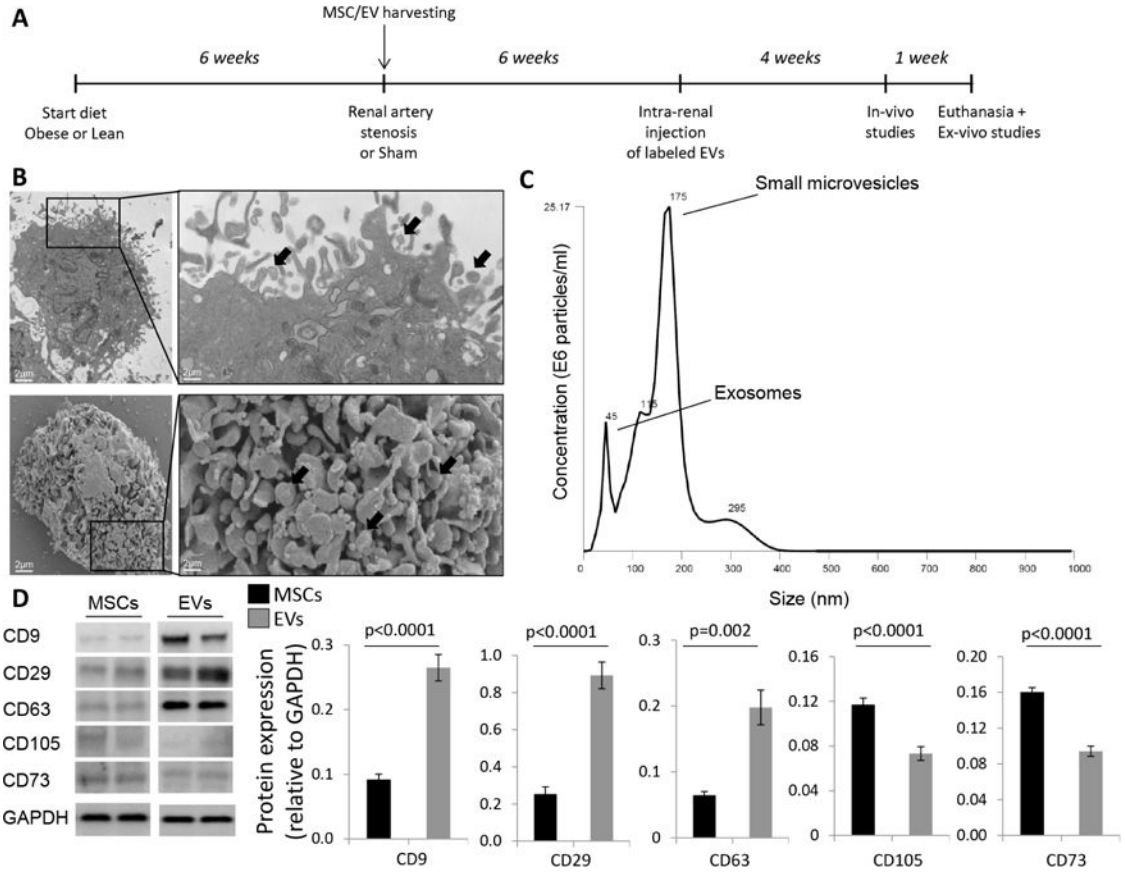

Figure 1. Cultured porcine MSCs release EVs

A: Schematic of the experimental protocol. B: Transmission (top) and scanning (bottom) electron microscopy showing that cultured MSCs release substantial amounts of EVs (black arrows). C: Size distribution of isolated EVs. D: EVs expressed common EV and MSC markers.

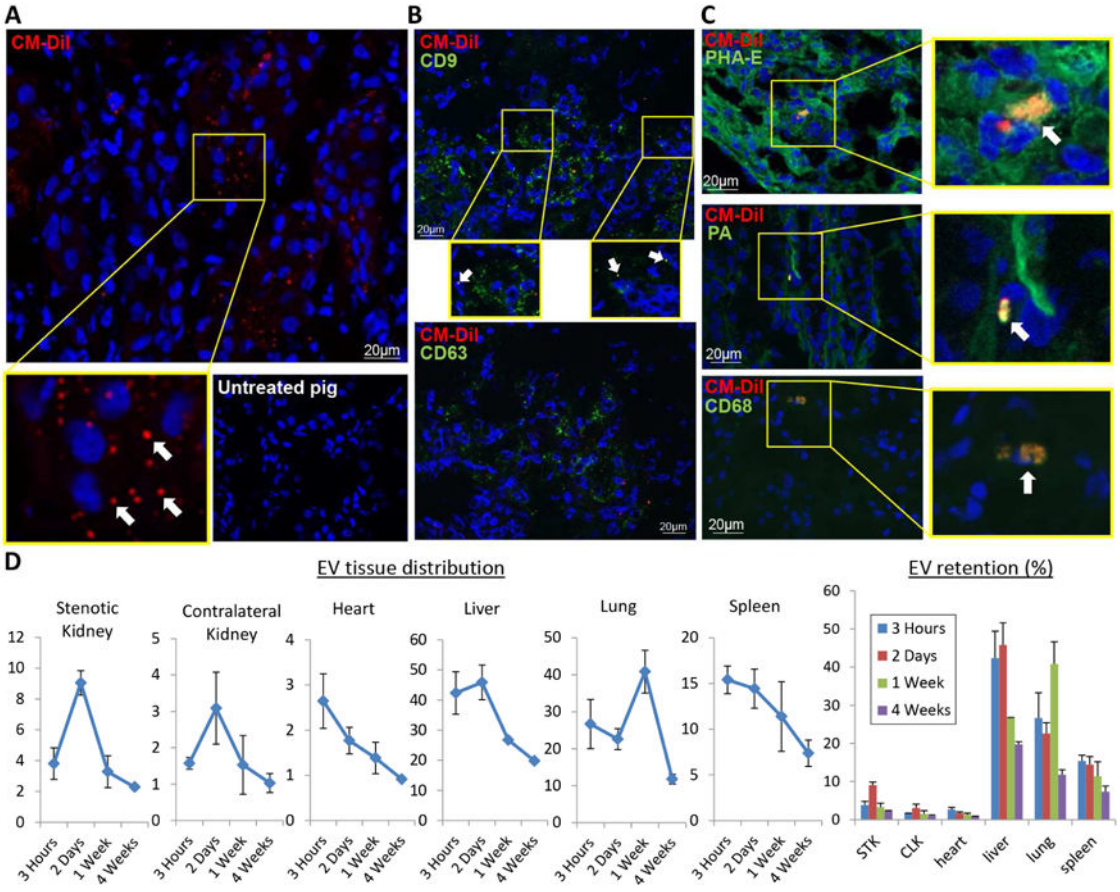

Figure 2. EV membrane fragments were retained within some organelles of renal cells and macrophages

A: Fragments of red immunofluorescent stained EVs (PKH26, arrows, 40X) were detected in the stenotic kidney 4 weeks after administration (top), whereas untreated stenotic kidneys did not show any fluorescent red signals (bottom). DAPI=blue, nuclei. B: Immunofluorescent co-staining with phaseolus vulgaris erythroagglutinin (PHA-E), peanut agglutinin (PA), and CD68 identified EV fragments within proximal tubular cells, distal tubular cells, and macrophages, respectively. D: Labeled EVs were tracked in frozen sections from the heart, lungs, liver, spleen, and both kidneys, and their retention calculated and expressed as % of injected amount.

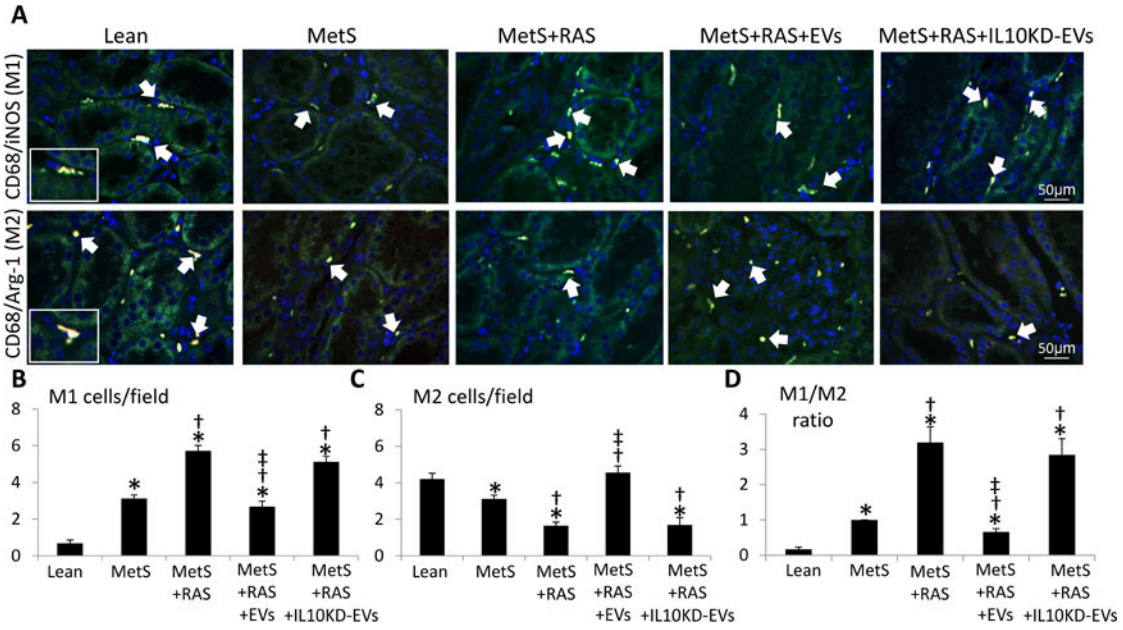

Figure 3. EVs induce a shift in renal macrophage phenotype

Representative images (X40) of immunofluorescence staining for stenotic kidney M1 [CD68 (red)/inducible nitric oxide synthase (green)] and M2 [CD68/arginase-1 (green)] macrophages (double staining yellow). Quantification of stenotic-kidney M1 and M2 macrophages and M1/M2 ratio. *p<0.05 vs. Lean; †p<0.05 vs. MetS; ‡p<0.05 vs. MetS +RAS.

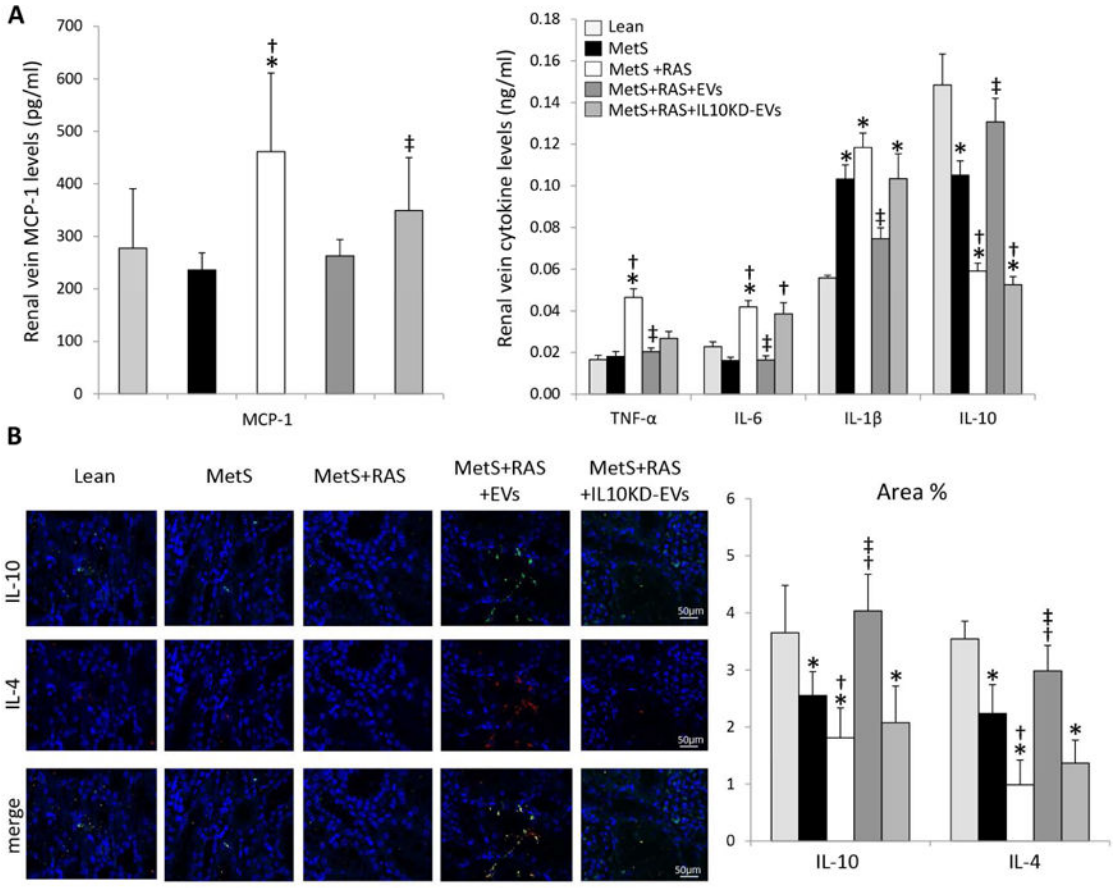

Figure 4. MSC-derived EVs ameliorate renal inflammation

A: Renal-vein levels of monocyte-chemoattractant protein (MCP)-1, tumor necrosis factor (TNF)-α, interleukin (IL)-6, IL-1β, and IL-10. B: Representative kidney IL-10 and IL-4 staining and its quantification. *p<0.05 vs. Lean; †p<0.05 vs. MetS; ‡p<0.05 vs. MetS +RAS.

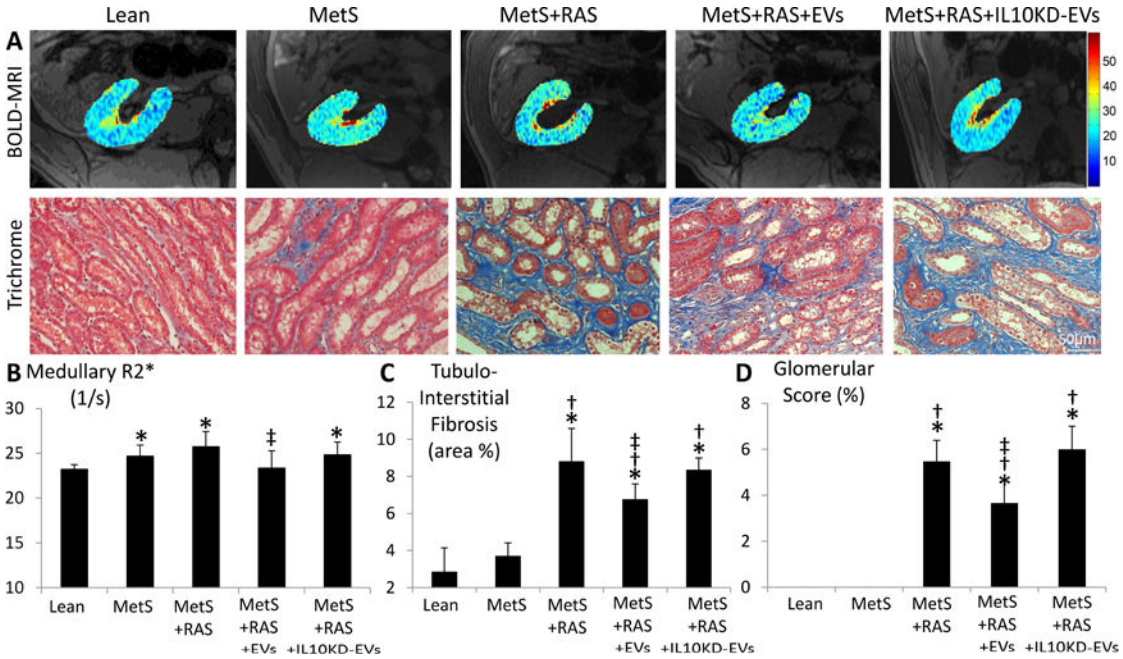

Figure 5. EVs ameliorate renal hypoxia and scarring

A: Representative kidney blood-oxygen-level-dependent magnetic-resonance images and trichrome staining. Quantifications of medullary red hypoxic regions (R2* index) (B), tubulointerstitial fibrosis (C), and glomerular score (D). *p<0.05 vs. Lean; †p<0.05 vs. MetS; ‡p<0.05 vs. MetS+RAS.

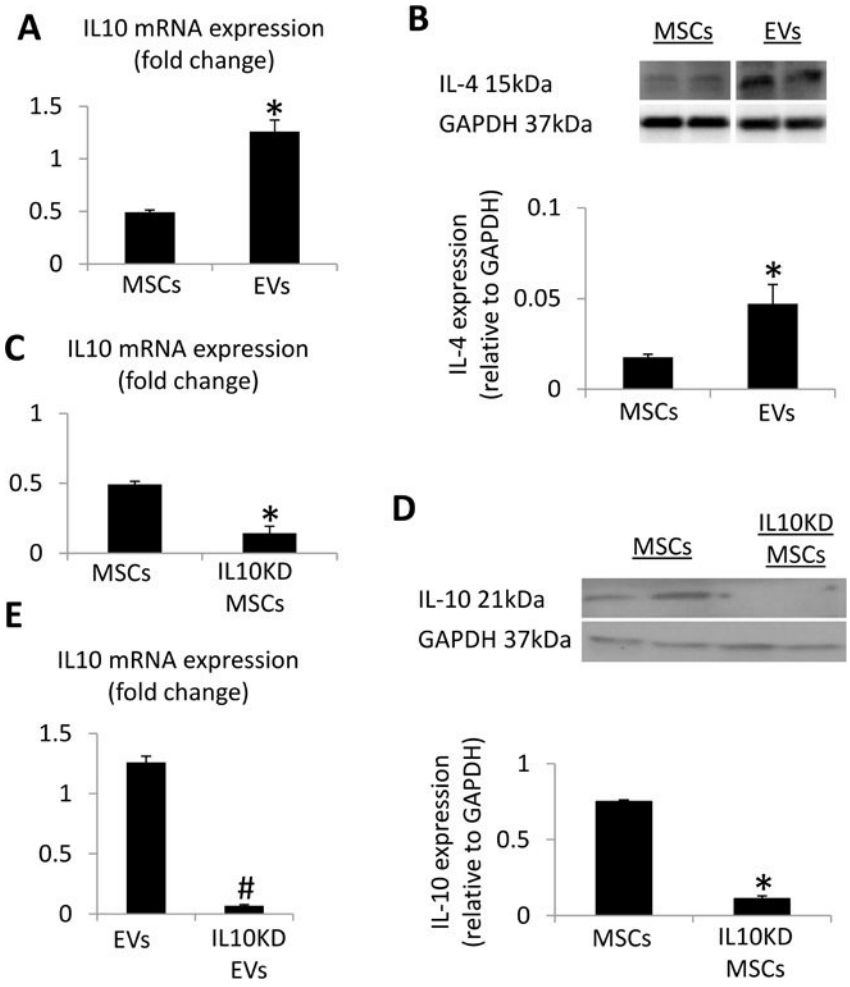

Figure 6. IL10 knockdown (IL10KD)

A: Interleukin (IL)-10 mRNA expression was enriched in EVs compared to MSCs. B: IL-4 protein expression was enriched in EVs compared to MSCs. IL10KD in MSCs using small-interfering RNA induced a significant decrease in IL-10 mRNA (C) and protein (D) compared to untreated MSCs. E: IL-10 mRNA expression was downregulated in EVs derived from IL10KD MSCs compared to EVs derived from untreated MSCs. *$p<0.05$ vs. MSCs, #$p<0.05$ vs. EVs.

Table 1

Systemic characteristics and single-kidney function in study groups at 16 weeks.

	Lean	MetS	MetS+RAS	MetS+RAS+EVs	MetS+RAS+IL10KD EVs
Body weight (Kg)	71.1±4.0	93.4±0.9 *	92.4±2.3 *	90.6±3.1 *	86.9±3.0 *
MAP (mmHg)	102.8±3.6	124.2±4.0 *	128.8±6.7 *	120.0±3.4 *	116.9±3.9 *
Degree of stenosis (%)	0	0	61.4±7.6 *	61.3±4.3 *	68.0±6.4 *
Total cholesterol (mg/dl)	82.5 (76.0–90.5)	347.0 (330.0–517.5) *	390.0 (336.0–426.0) *	413.0 (315.5–529.8) *	420.0 (323.5–534.0) *
Triglycerides (mg/dl)	8.0 (5.8–11.3)	14.0 (13.0–25.5) *	13.0 (5.0–20.0) *	14.5 (8.3–16.8) *	13.0 (10.5–18.0) *
HDL cholesterol (mg/dl)	47.0 (42.5–52.5)	140.0 (110.5–167.0) *	110.0 (98.0–172.0) *	126.0 (106.0–166.8) *	107.0 (104.0–154.0) *
LDL cholesterol (mg/dl)	33.4±6.5	398.4±140.4 *	319.6±128.5 *	314.3±119.6 *	416.4±114.3 *
Fasting insulin (μU/ml)	0.4 (0.3–0.5)	0.7 (0.7–0.8) *	0.7 (0.7–0.8) *	0.7 (0.7–0.8) *	0.7 (0.7–0.8) *
HOMA-IR score	0.6 (0.6–0.7)	1.9 (1.4–1.9) *	1.9 (1.8–2.0) *	1.9 (1.7–2.0) *	1.9 (1.8–2.0) *
Fasting glucose (mg/dl)	129.5±36.1	116.2±22.7	112.1±27.6	103.5±28.3	124.8±36.7
Serum creatinine (mg/dl)	1.47±0.23	1.54±0.18	1.77±0.23 *†	1.45±0.37 ‡	1.92±0.19 *
PRA (ng/ml/h)	0.14±0.09	0.15±0.08	0.21±0.11	0.14±0.12	0.15±0.17
Renal volume (ml)	137.2±6.4	217.9±7.4 *	182.4±8.8 *†	207.4±29.1 *‡	189.3±15.6 *
RBF (ml/min)	502.1±27.4	848.6±76.1 *	628.5±27.5 *†	866.1±104.1 *‡	447.8±85.2 †‡
GFR (ml/min)	76.0±4.0	142.6±7.3 *	100.3±7.1 *†	128.7±13.6 *‡	82.7±12.5 †

IL10KD: Interleukin-10 knockdown; MAP: Mean arterial pressure; PRA: Plasma renin activity; HDL: high-density lipoprotein; LDL: low-density lipoprotein; HOMA-IR: homeostasis model assessment of insulin resistance, RBF: renal blood flow; GFR: glomerular filtration rate.

* $p<0.05$ vs. Lean;

† $p<0.05$ vs. MetS;

‡ $p<0.05$ vs. MetS+RAS